Published in final edited form as:
J Proteome Res. 2012 May 4; 11(5): 2996–3003. doi:10.1021/pr300111x.

NMR metabolomics of MTLn3E breast cancer cells identifies a role for CXCR4 in lipid and choline regulation

Louic S. Vermeer[1,*], **Gilbert O. Fruhwirth**[2], **Pahini Pandya**[1], **Tony Ng**[2], and **A. James Mason**[1,*]

[1]Institute of Pharmaceutical Science, King's College London, Franklin-Wilkins Building, 150 Stamford Street, London SE1 9NH, UK

[2]Richard Dimbleby Department of Cancer Research, Division of Cancer Studies and Randall Division of Cell & Molecular Biophysics, King's College London, Guy's Medical School Campus, London SE1 1UL, UK

Abstract

The alpha chemokine receptor CXCR4 is up-regulated in certain types of breast cancer. Truncation of the C-terminus of this receptor alters cell morphology and increases invasiveness and metastatic potential. Here, to better understand the effects of CXCR4 expression and truncation in breast cancer cells, we have used high resolution magic angle spinning (HR-MAS) NMR studies of rat breast carcinoma MtLn3E cells to characterise the metabolite complement of cells heterologously expressing human CXCR4 or its C-terminal truncation mutant, Δ34-CXCR4. Notable reductions in choline levels were detected when either cells expressing wild-type CXCR4 or Δ34-CXCR4 were compared with cells containing an empty expression vector. Cells expressing CXCR4-Δ34 had reduced lipid content when compared with either the wild-type CXCR4 expressing cells or those containing the empty expression vector. Taken together, our results show that distinct effects on the metabolite complement can be linked to either CXCR4 expression or CXCR4 regulation. The metabolite markers for these two effects identified in the present study can, in turn, be used to further investigate the role of CXCR4 in metastasis.

[*]Corresponding authors: Institute of Pharmaceutical Science, King's College London, Franklin-Wilkins Building, 150 Stamford Street, London SE1 9NH; Tel: + 44 207 848 4813; Fax: + 44 207 848 4800; louic.vermeer@kcl.ac.ukjames.mason@kcl.ac.uk.
Contributions: LSV, GOF, TN and AJM designed the research. GOF and TN provided cell lines. PP and GOF prepared cell samples. LSV and PP performed the NMR experiments. LSV wrote the analysis software and performed statistical analysis. LSV, GOF, and AJM wrote the manuscript.

Supporting Information Available: Included are: results of the permutation tests, figures describing the assignment of key resonances and description of primers and FACS analysis of the cell lines. This material is available free of charge via the Internet at http://pubs.acs.org

Europe PMC Funders Author Manuscripts

Europe PMC Funders Author Manuscripts

Graphical Abstract

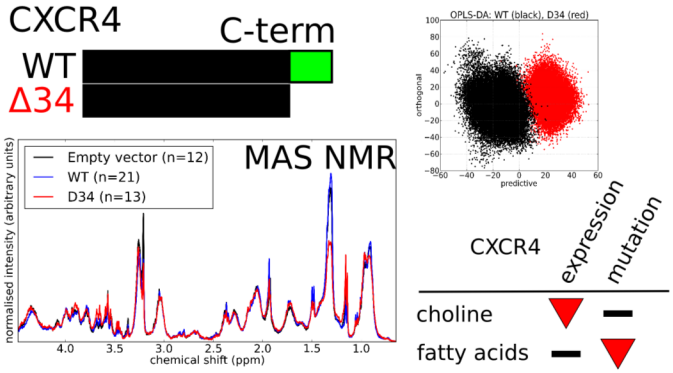

Keywords

NMR metabolomics; High resolution magic angle spinning (HR-MAS); CXCR4; breast cancer cells

Introduction

The 352 amino acid CXC chemokine receptor type 4 (CXCR4) selectively binds the CXC chemokine stromal cell-derived factor-1 (SDF-1) also known as CXCL12. This G-protein coupled receptor (GPCR) is implicated in a variety of human diseases; it serves as a coreceptor for entry of T-tropic HIV viruses that target CD4-positive T-cells,[1,2] was found to be expressed in >20 types of human cancers[3,4] and has been linked to enhanced cancer cell motility and metastasis. In particular, an important role for CXCR4 has been demonstrated in breast cancer metastasis where signalling through CXCR4 leads to actin polymerization, formation of pseudopodia, chemotaxis, and increased metastasis in cancer cells.[5] The C-terminus of CXCR4 is crucial to this activity and expression of a C-terminal truncation mutant in MCF-7 cells was shown to lead to altered cell morphology, higher growth rate, and increased cell motility, when compared with wild type CXCR4 or vector transduced cells.[6] Recent results also show that the truncation of the C-terminus of CXCR4 leads to increased invasive potential of mammary carcinoma cells *in vitro* in a MatriGel invasion assay and increased metastatic potential *in vivo* in a murine model of spontaneous breast cancer metastasis.[7] This behaviour is likely to be linked to the substantially reduced receptor internalization and hence degradation observed in cells expressing the truncated CXCR4.[7] Although CXCR4 truncation mutations have been found to play an important role in Warts, Hypogammaglobulinemia, Infections and Myelokathexis (WHIM) syndrome,[8,9] as yet, no such deletions have been observed in cancer. Nevertheless, different CXCR4 mutations have been reported in a number of cancers and are implicated in promoting CXCR4 persistence at the cell surface and/or conferring migratory advances to the cell lines established from these cancers.[10-12]

Magnetic resonance spectroscopy (MRS) has been shown to have potential in providing information about tumour phenotypes in human samples *in vivo*. For instance, it has been used to distinguish tumour tissue from non-lactating human breast tissue[13-15] and for the evaluation of human breast lesions. Furthermore, the composite total choline resonance in proton spectra was used to distinguish malign from benign tissue[17,18] and for monitoring the success of neoadjuvant chemotherapy in locally advanced human breast cancer[19].

In order to gain insight into the metabolic changes associated with increased CXCR4 expression or truncation of its C-terminus, we have characterized the changes in the small molecule complement of a breast cancer cell model designed to distinguish CXCR4-induced changes and truncation-induced alterations. Specifically, we applied high resolution magic angle spinning (HR-MAS) NMR techniques to lyophilised and rehydrated rat mammary adenocarcinoma MTLn3E cells, either transduced with an empty vector or stably expressing either wildtype or C-terminally truncated CXCR4.

Materials and Methods

Cloning, generation of stable cell lines, and cell culture

The DNA of the wild-type human chemokine receptor CXCR4 (WT-CXCR4) was amplified by PCR. In the case of the truncation mutant (Δ34-CXCR4), a deletion of the last 34 amino acids of the C-terminus of CXCR4 was achieved by PCR amplification of the human CXCR4 receptor with appropriate primers for the wildtype N-terminus and the truncated C-terminus (Table S1, Supporting Information). Subsequently, both coding sequences were subcloned between the *HindIII* and *EcoR1* sites of pEGFP-N1 (Clontech, Saint-Germain-en-Laye, France) yielding C-terminal GFP fusion proteins of wildtype and mutant CXCR4. These C-terminal fusion proteins were then subcloned into the retroviral expression vector pLPCX (Clontech, Saint-Germain-en-Laye, France). All constructs were confirmed by sequence analysis and retroviruses were produced by standard techniques. Rat mammary adenocarcinoma cells (MTLn3E) were infected with retroviruses for the transduction of either WT-CXCR4-GFP, Δ34-CXCR4-GFP, or the empty vector. Stably expressing cells were generated after infection by selection with puromycine (1 μg/ml). Subsequently, FACS-sorting was performed to obtain single clones with comparable expression levels (Fig. S1, Supporting Information). One single clone per cell line was selected and used for all further experiments. All cell lines were cultured in αMEM supplemented with 5% foetal bovine serum, penicillin/streptomycin (100 IU), and *L*-glutamine in an atmosphere containing 5% CO_2 (v/v) in the presence of puromycin.

Preparation of cell samples for NMR

On the day before the experiment, the indicated stable cell lines were plated at a density of 50,000 cells per cm^2 in 10 cm Petri dishes (Nunc/Fisher Scientific, Loughborough, UK). After incubation overnight, the culture media were refreshed. Cells were once washed with ice-cold phosphate buffered saline lacking calcium and magnesium (PBS, pH = 7.4), then scraped in ice-cold PBS, centrifuged at 200 g for 4 min, and re-suspended in 0.5 ml ice-cold PBS before being transferred to sterile 1.5 ml tubes. Cell suspensions were centrifuged again at 200 g for 5 min and the pellets were immediately snap-frozen in liquid nitrogen. Frozen cell pellets were stored at −80°C until lyophilisation which was carried out on the same day as harvesting the cells. Preceding NMR measurements, the samples were inserted into Bruker KelF MAS rotor inserts and rehydrated for 60 minutes with 30 μl D_2O at room temperature. Shorter rehydration times led to larger spectral linewidths that were attributed to incomplete rehydration. All reagents used were analytical grade or better.

Cell handling and storage for metabolomics research by HR-MAS has been investigated systematically.[20] It was shown that freezing cells without a cryo-preservative lyses 100% of the cells, increasing metabolite visibility. Furthermore, the lysed cells showed significant differences in the lipid profiles when compared with intact cells. Duarte *et al.* therefore emphasize that reproducibility of particularly the lysis procedure is critical, especially when the lipid composition is of interest. Because the percentage of broken cells may vary, and cells have been shown to break as a result of sample handling or MAS, we decided to use

freeze-drying to reproducibly break 100% of the cells. The samples thus obtained led to HR-MAS spectra of good quality (Fig. 1).

NMR acquisition and processing

HR-MAS NMR spectra were recorded on a Bruker Avance 400 MHz spectrometer equipped with an HR-MAS probe using a CPMG solid echo pulse sequence. The spinning speed was 5 kHz. A CPMG echo time of 190 μs was used, and the ^{1}H 90 degree pulse was 10 μs. The signal of residual water was suppressed using continuous wave pre-saturation during the relaxation delay of 1 second. Spectra were recorded at 310 K and spectra of sufficient signal to noise were obtained in less than 30 minutes. To help in the assignment of the metabolite resonances, J-resolved, COSY and ^{1}H-^{13}C-HSQC spectra were recorded for some of the samples, using default pulse sequences as provided by Bruker. The acquisition of these two dimensional spectra took less than 24 hours.

Multivariate analysis

Pre-processing and orthogonal projection to latent structures discriminant analysis (OPLS-DA) were carried out with software that was developed in our lab using the python programming language with numpy and scipy for calculations, and matplotlib for visualization. Although metabolomics software exists (SIMCA, pirouette, MATLAB programmes), we could not identify a software package that allowed us to import the Bruker NMR spectra and subsequently apply all the pre-processing, analysis, and cross-validation methods described here. The non-linear iterative partial least squares (NIPALS) algorithm[21] was used for OPLS-DA[22,23] analysis, implemented according to the references given.

Spectra were calibrated to the alanine doublet at 1.50 ppm. Regions above 4.48 ppm and below 0.65 ppm were excluded because they contained mostly noise, the water peak or the TSP reference signal (which we did not use for referencing), leaving 6106 data points per spectrum. Spectra were normalized using probabilistic quotient normalization,[24] where the median of the spectra from the reference sample was used as reference spectrum. The reference spectra were either those from cells transfected with the empty vector, or those without a mutation, depending on the comparison that is being made. Spectra were auto-scaled (variance of every datapoint normalized to 1), and both normalization and autoscaling were included in the cross-validation.

A 4-fold cross-validation was carried out, [25] meaning that 25% of the samples were used as a test set, and 75% as training set, ensuring that the number of samples in the test set was proportional to the total number of samples from each class, and that at least one sample from each class was present in the test set. As validation set (to choose the number of components in the model) a minimum of one sample per class was left out of the training set. When the number of samples in the two classes was not equal, one sample was of the set with the lowest number of samples, and proportionally more samples were left out of the larger set. The number of components was then determined by the F1-score with the constraint that the maximum number of components to use was 6. This procedure was repeated 2000 times with randomly chosen samples in the test set and validation set, to prevent bias due to an unlucky choice of training/validation/test set. Therefore a total of 4 × 2000 models was generated. The number of components chosen in each of the models is given in the supplementary material. The chosen number of components minus one was then used as an OPLS filter, and a PLS-DA analysis with two components was carried out on the filtered data to yield one predictive and one orthogonal component. To verify our classification against a random one, 2000 runs were carried out with permutated class assignments (Fig. S2-4, Supporting Information). Back-scaled loadings[35] were used to

Europe PMC Funders Author Manuscripts

identify resonances with high variance and high weight, and verified against the peak intensity and standard error of the original spectra after PQN normalisation.

Peaks were assigned (see Supporting Information, Fig. S5-7) by comparing chemical shift values, multiplicities from J-resolved NMR spectra, and ^{13}C chemical shifts from $^{1}H/^{13}C$ HSQC NMR spectra to values from the literature,[26,27] the BMRB[28] and HMDB,[29] and statistical total correlation spectroscopy (STOCSY) was used to help in the assignment (Fig. S8).[30]

Results and Discussion

Experimental design

The role of CXCR4 in mediating breast cancer cell signalling and motility can be considered in terms of the changes in effector molecules that occur as a result of changes in its expression or activity. This in turn is dependent on obtaining an accurate overview of the key changes in the cellular metabolite complement. A variety of metabolomic methodologies exist for such purposes but many require the laborious and time consuming preparation of perchloric acid extracts, a process which leads to possible modification of metabolite composition.[26,31,32] Here we have used an HR-MAS NMR approach with the aim of minimising such problems. Specifically, we have studied rat MTLn3E cells that have been mechanically dislodged from the surface of their culture vessels and immediately snap-frozen before being lyophilised, transferred to MAS rotors and rehydrated with D2O before measurement. Snap-freezing lyses cells completely, enhances metabolites visibility but also alters the lipid profile compared with intact cells.[20] Magic angle spinning NMR mechanically introduces rapid re-orientation into semi-solid samples, reducing contributions from anisotropic interactions and improving spectral resolution. As described previously, this provides enhanced information on lipids without notable losses of information for smaller metabolites.[20] The overall process allows ^{1}H NMR spectra of sufficient quality to be reproducibly obtained (Fig. 1) enabling the subsequent analysis described here.

The present study has been performed in the absence of CXCL12, the ligand for CXCR4, and hence is focussed on differences due to CXCR4 expression and ligand independent regulation rather than ligand-dependent signalling. We used CXCR4 that was fused with its C-terminus to green fluorescent protein (GFP). This modification has been shown not to affect CXCR4 signalling and/or trafficking.[33,34] MTLn3E cells were found not to express CXCR4 (Fig. S1, Supporting Information), which makes them a good model system for studying CXCR4-induced metabolic changes. We generated cell lines stably expressing either wildtype WT-CXCR4-GFP, the truncation mutant Δ34-CXCR4-GFP, or the empty vector via retroviral infection, selection, and fluorescence-activated cell sorting (FACS) of GFP expressors to obtain single clones. We expanded single clones with almost identical expression profiles and used them for all experiments (Fig. S1, Supporting Information). Important differences in the invasive and metastatic potential of MTLn3E cells expressing either WT-CXCR4-GFP or Δ34-CXCR4-GFP have been described recently.[7] Cells stably expressing the truncation mutant receptor invade significantly more through Matrigel as cells stably expressing the wildtype receptor.[7] This effect is evident at basal conditions (no ligand present) and the difference increases with addition of the chemokine ligand CXCL12. FBS was added in one experiment that served as a positive control and under these conditions the mutant also shows increased invasiveness. Cells stably expressing the truncation mutant receptor were also more invasive *in vivo*.[7]

In order to discriminate differences due to expression of either wildtype CXCR4, truncated CXCR4, or the empty vector, the metabolite complement of three different samples was compared using orthogonal projection to latent structures discriminant analysis (OPLS-DA).

By comparing cells stably expressing either the empty vector or WT-CXCR4-GFP, metabolic changes that occur as a result of CXCR4 expression can be assessed, serving as a model for CXCR4 over-expression in cancer cells. In contrast, a comparison of cells stably expressing WT-CXCR4-GFP and Δ34-CXCR4-GFP will give information on metabolic changes that are related to the truncation of the CXCR4 C-terminus, which is responsible for the receptor down-modulation and is also important in the WHIM syndrome. MTLn3E cells infected with the empty vector were also compared to those stably expressing Δ34-CXCR4-GFP, and any observed metabolic differences must therefore be related to expression of the truncation mutant.

A visual inspection of the averaged and normalized HR-MAS spectra (Fig. 1) suggests that there are differences in the region around 1.33 ppm, 3.21 ppm and 3.66 ppm. The statistical validation of these differences is discussed below and in the materials and methods section.

Multivariate analysis

Previous work assessing the effects of cell handling and storage on cell integrity indicated that snap-freezing and consequent lysis of mammalian cells leads to an increase in detected choline, phosphocholine and glycerophosphocholine and a decrease in detected phosphatidylcholine relative to intact cells.[20] Although each of our cell preparations was treated in the same way, a thorough statistical analysis is warranted in order to ensure the absence of artefacts. Figure 2 shows the cross-validated scores all models generated as specified in the materials and methods section. In Figure 2A and 2B, cells expressing the empty vector and cells expressing WT-CXCR4-GFP, respectively, are compared to cells that express C-terminal truncated Δ34-CXCR4-GFP. A good separation between the two sample types is obtained in both cases. The good separation of the data points in each class indicate that the predictive component scores lead to a predominantly successful classification of the two samples. Interestingly, Figure 2C shows that the differences between NMR spectra of cells expressing the empty vector and cells expressing WT-CXCR4-GFP appear to be less pronounced. The data indicate that truncation of the CXCR4 C-terminus by 34 residues results in changes of the metabolic state of MTLn3E cells that allow these mutant receptor expressing cells to be easily distinguished from cells expressing either the wildtype receptor or the empty vector on the basis of their NMR spectra. Expression of the wildtype receptors also induces differences in the metabolome of MTLn3E cells, but these differences appear to be smaller as indicated by the larger overlap between the two groups on the cross-validated scores plot (compare Fig. 2B with Fig. 2C).

Assignment of discriminating metabolites

The back-scaled loadings[35] represent the covariance matrix of the spectra (Fig. 3). The normalised weights from the OPLS model are represented as a colour, and indicate the importance of each region in the predictive model. Both the loadings and weights are averaged over all of the models that were calculated during cross-validation. Consequently, any variation that depends on the choice of the training set is averaged out. Peaks on the red side of the colour spectrum indicate the resonance frequencies of metabolites that distinguish the two cell types from each other. The peaks that have been assigned to fatty acids (1.33 ppm; Fig. S5 Supporting Information), choline (3.21 ppm; Fig. S6) and the region around 3.66 ppm (Fig. S7) are clearly visible and show both a high covariance and high weight, indicating their importance in distinguishing between the cell types under comparison.

CXCR4 expression reduces the choline levels in breast cancer cells

Cells that express either WT-CXCR4-GFP or Δ34-CXCR4-GFP have lower relative concentrations of choline than cells that were expressing only the empty vector, indicating

that expression of CXCR4 (with or without its C-terminus) lowers the relative choline concentration in MTLn3E cells in the absence of the CXCR4 ligand (Fig. 4B). Figure 4B shows the intensity of the peak in the NMR spectrum at 3.21 ppm, which we assigned to choline on the basis of its chemical shift, the HSQC (Fig. S6) and STOCSY correlations (Fig. S8) with the α-CH_2 of choline at 4.06 ppm and a peak at 3.23 ppm[26]. In contrast, the relative intensity of the choline peak is not significantly different when WT-CXCR4-GFP or Δ34-CXCR4-GFP expressing cells are compared, adding further support to the above observation.

Effect of CXCR4 truncation

The fatty acid content is lower in cells that express the truncation mutant as judged by the peak intensity at 1.33 ppm (Fig. 4A). This peak was assigned as described above and has STOCSY correlations with peaks at 0.91, 1.59 and 2.04 ppm (Fig. S8) which are all attributable to fatty acids. Importantly, no significant changes in the total fatty acid content are observed when cells containing the empty vector are compared with cells expressing WT-CXCR4 (Fig. 4A/C) indicating that the observed changes in lipid metabolism are exclusively a result of expression of truncated CXCR4.

In the same cell types, an increase of multiple peak intensities between 3.63 and 3.71 ppm are observed (Fig. 4C). The standard error of the spectra obtained for Δ34-CXCR4-GFP expressing cells appears to be rather high (Figure 4C), but the average backscaled loadings and weights indicate that these observed differences are not due to random variation. The peak at 3.66 ppm has STOCSY correlations (Fig. S8) with peaks at 3.59 and 3.80-3.84 ppm. These peaks cannot be unambiguously assigned however, due to overlapping resonances in this region of the spectrum, but through comparison with literature values[27] can be tentatively assigned to glycerophosphocholine. If genuine, this would indicate that the changes in fatty acid content observed are, more precisely, changes in glycerophospholipid metabolism.[36,37]

Relevance of choline and lipid metabolism to breast cancer

Over-expression of CXCR4 has been shown to correlate with increased metastatic potential[4] and poor prognosis in several types of cancer[3] including breast cancer.[5] Recently, it has been suggested that mutations that lead to reduced CXCR4 degradation, and that may only be apparent in cells homozygous for the mutation, may be implicated in promoting invasion and metastasis in a variety of cancers.[7] We have set out to study the metabolomic changes induced by expression of both wildtype and C-terminal truncated CXCR4 in a metastatic breast cancer cell line normally having undetectable levels of CXCR4 (by flow cytometry, see Fig. S1). MRS experiments of cell cultures, biopsies, and *in vivo* have been used to identify biomarkers for cancer, characterise cancers, and as a diagnostic tool.[38] Indeed NMR has been used to identify metabolomic changes between metastatic, non-metastatic, and normal cell lines and Morse et al[36] found a significant decrease of total choline levels in metastatic and non-metastatic breast cancer cells as compared to non-tumourigenic breast cells. Our finding of reduced total choline levels upon CXCR4 expression (either wildtype or Δ34 truncation mutant) is in agreement with these reports in that our cell model is also being rendered more motile by expression of CXCR4.[4,6]

Truncation of the CXCR4 C-terminus has been linked to sustained signalling, enhanced cell motility, invasiveness and metastatic potential.[6,7] A relative increase in the region between 3.20 and 3.25 ppm is consistently observed in malignant breast cancers,[17,36,38] and can be assigned to either total choline containing metabolites, choline, phosphocholine, or glycerophosphocholine. Furthermore, it has been shown that cell extracts of malignant breast cancer cells (MDA-MB-231) contained higher concentrations of phosphocholine,

lysophosphatidylcholine, glycerophosphocholine and glycerol 3-phosphate as compared to non-metastatic (MCF-7) breast cancer cells or non-tumorigenic but immortal cells (MCF-10A) and the authors suggested the involvement of phospholipases.[36] However, a different group found no evidence for phospholipase A2-mediated catabolism in the metastatic human breast cancer cell line MDA-MB-231.[37]

In the present study no differences in choline content could be detected as a result of truncation of the CXCR4 C-terminus but, interestingly, differences in lipid content were indeed apparent. The results from our HR-MAS metabolomics analysis indicate therefore, that expression, combined with dysregulation, of CXCR4 causes substantial and detectable changes in lipid metabolism. To the best of our knowledge, this is the first time that the link between CXCR4 and lipid metabolism has been made on a metabolomics level.

Together with the described HR-MAS NMR approach, which allows observation of lipid signals which is not possible in perchloric acid extracts,[26] the present model system will allow further investigation of the important role of wildtype and mutant CXCR4 expression, activation and regulation thereby allowing insight into CXCR4-related human diseases, including cancer and WHIM syndrome, on a metabolomic level.

Supplementary Material

Refer to Web version on PubMed Central for supplementary material.

Acknowledgments

This work was supported by the Medical Research Council (NIRG G0801072/87482 to AJM) and the Wellcome Trust (VIP Award to AJM and Capital Award for the KCL Centre for Biomolecular Spectroscopy). The authors thank Jane Hawkes and Dr Andrew Atkinson for their support with NMR experiments.

REFERENCES

1. Gupta SK, Pillarisetti K. Cutting edge: CXCR4-Lo: molecular cloning and functional expression of a novel human CXCR4 splice variant. J. Immunol. 1999; 163(5):2368–72. [PubMed: 10452968]
2. Caruz A, Samsom M, Alonso JM, Alcami J, Baleux F, Virelizier JL, Parmentier M, Arenzana-Seisdedos F. Genomic organization and promoter characterization of human CXCR4 gene. FEBS Lett. 1998; 426(2):271–8. [PubMed: 9599023]
3. Sun X, Cheng G, Hao M, Zheng J, Zhou X, Zhang J, Taichman RS, Pienta KJ, Wang J. CXCL12 / CXCR4 / CXCR7 chemokine axis and cancer progression. Cancer Metastasis Rev. 2010; 29(4): 709–22. [PubMed: 20839032]
4. Busillo JM, Benovic JL. Regulation of CXCR4 signaling. Biochim. Biophys. Acta. 2007; 1768(4): 952–63. [PubMed: 17169327]
5. Muller A, Homey B, Soto H, Ge N, Catron D, Buchanan ME, McClanahan T, Murphy E, Yuan W, Wagner SN, Barrera JL, Mohar A, Verastegui E, Zlotnik A. Involvement of chemokine receptors in breast cancer metastasis. Nature. 2001; 410(6824):50–6. [PubMed: 11242036]
6. Ueda Y, Neel NF, Schutyser E, Raman D, Richmond A. Deletion of the COOH-terminal domain of CXC chemokine receptor 4 leads to the down-regulation of cell-to-cell contact, enhanced motility and proliferation in breast carcinoma cells. Cancer Res. 2006; 66(11):5665–75. [PubMed: 16740704]
7. Fruhwirth, GO.; Brock, A.; Keppler, M.; Khan, A.; Giampieri, S.; Sahai, E.; Gillet, C.; Ameer-Beg, S.; Archibald, SJ.; Ng, T. Receptor dimerization and degradation dampen the pro-metastatic effect of mutated CXCR4. submitted for publication
8. Diaz GA. CXCR4 mutations in WHIM syndrome: a misguided immune system? Immunol. Rev. 2005; 203:235–43. [PubMed: 15661033]

9. Balabanian K, Lagane B, Pablos JL, Laurent L, Planchenault T, Verola O, Lebbe C, Kerob D, Dupuy A, Hermine O, Nicolas JF, Latger-Cannard V, Bensoussan D, Bordigoni P, Baleux F, Le Deist F, Virelizier JL, Arenzana-Seisdedos F, Bachelerie F. WHIM syndromes with different genetic anomalies are accounted for by impaired CXCR4 desensitization to CXCL12. Blood. 2005; 105(6):2449–57. [PubMed: 15536153]
10. Chabot DJ, Zhang PF, Quinnan GV, Broder CC. Mutagenesis of CXCR4 identifies important domains for human immunodeficiency virus type 1 X4 isolate envelope-mediated membrane fusion and virus entry and reveals cryptic coreceptor activity for R5 isolates. J. Virol. 1999; 73:6598–6609. [PubMed: 10400757]
11. Ierano C, Giuliano P, D'Alterio C, Cioffi M, Mettivier V, Portella L, Napolitano M, Barbieri A, Arra C, Liguori G, Franco R, Palmieri G, Rozzo C, Pacelli R, Castello G, Scala S. A point mutation (G574A) in the chemokine receptor CXCR4 detected in human cancer cells enhances migration. Cell Cycle. 2009; 8:1228–1237. [PubMed: 19305148]
12. Schüller U, Koch A, Hartmann W, Garrè ML, Goodyer CG, Cama A, Sörensen N, Wiestler OD, Pietsch T. Subtype-specific expression and genetic alterations of the chemokinereceptor gene *CXCR4* in medulloblastomas. International Journal of Cancer. 2005; 117:82–89.
13. Kvistad KA, Bakken IJ, Gribbestad IS, Ehrnholm B, Lundgren S, Fjosne HE, Haraldseth O. Characterization of neoplastic and normal human breast tissues with *in vivo* (^{1})H MR spectroscopy. J. Magn. Reson. Imaging. 1999; 10(2):159–64. [PubMed: 10441019]
14. Thomas MA, Wyckoff N, Yue K, Binesh N, Banakar S, Chung HK, Sayre J, DeBruhl N. Two-dimensional MR spectroscopic characterization of breast cancer in vivo. Technol Cancer Res. Treat. 2005; 4(1):99–106. [PubMed: 15649093]
15. Jacobs MA, Barker PB, Argani P, Ouwerkerk R, Bhujwalla ZM, Bluemke DA. Combined dynamic contrast enhanced breast MR and proton spectroscopic imaging: a feasibility study. J. Magn. Reson. Imaging. 2005; 21(1):23–8. [PubMed: 15611934]
16. Cecil KM, Schnall MD, Siegelman ES, Lenkinski RE. The evaluation of human breast lesions with magnetic resonance imaging and proton magnetic resonance spectroscopy. Breast Cancer Res. Treat. 2001; 68(1):45–54. [PubMed: 11678308]
17. Stanwell P, Gluch L, Clark D, Tomanek B, Baker L, Giuffre B, Lean C, Malycha P, Mountford C. Specificity of choline metabolites for in vivo diagnosis of breast cancer using ^{1}H MRS at 1.5 T. Eur. Radiol. 2005; 15(5):1037–43. [PubMed: 15351906]
18. Bolan PJ, Meisamy S, Baker EH, Lin J, Emory T, Nelson M, Everson LI, Yee D, Garwood M. *In vivo* quantification of choline compounds in the breast with ^{1}H MR spectroscopy. Magn. Reson. Med. 2003; 50(6):1134–43. [PubMed: 14648561]
19. Jagannathan NR, Kumar M, Seenu V, Coshic O, Dwivedi SN, Julka PK, Srivastava A, Rath GK. Evaluation of total choline from in-vivo volume localized proton MR spectroscopy and its response to neoadjuvant chemotherapy in locally advanced breast cancer. Br. J. Cancer. 2001; 84(8):1016–22. [PubMed: 11308247]
20. Duarte IF, Marques J, Ladeirinha AF, Rocha C, Lamego I, Calheiros R, Silva TM, Marques MP, Melo JB, Carreira IM, Gil AM. Analytical approaches toward successful human cell metabolome studies by NMR spectroscopy. Anal. Chem. 2009; 81(12):5023–32. [PubMed: 19462963]
21. Andersson M. A comparison of nine PLS1 algorithms. Journal of Chemometrics. 2009; 23:518–529.
22. Trygg J, Wold S. Orthogonal projections to latent structures (O-PLS). J. Chemometrics. 2002; 16:119–128.
23. Tapp HS, Kemsley EK. Notes on the practical utility of OPLS. Trends Anal. Chem. 2009; 28:1322–1327.
24. Dieterle F, Ross A, Schlotterbeck G, Senn H. Probabilistic quotient normalization as robust method to account for dilution of complex biological mixtures. Application in ^{1}H NMR metabonomics. Anal. Chem. 2006; 78(13):4281–90. [PubMed: 16808434]
25. Westerhuis JA, Hoefsloot HCJ, Smit S, Vis DJ, Smilde AK, van Velzen EJJ, van Duijnhoven JPM, van Dorsten FA. Assessment of PLSDA cross validation. Metabolomics. 2008; 4:81–89.
26. Sitter B, Sonnewald U, Spraul M, Fjosne HE, Gribbestad IS. High-resolution magic angle spinning MRS of breast cancer tissue. NMR Biomed. 2002; 15(5):327–37. [PubMed: 12203224]

27. Martinez-Bisbal MC, Marti-Bonmati L, Piquer J, Revert A, Ferrer P, Llacer JL, Piotto M, Assemat O, Celda B. ^{1}H and ^{13}C HR-MAS spectroscopy of intact biopsy samples *ex vivo* and *in vivo* ^{1}H MRS study of human high grade gliomas. NMR Biomed. 2004; 17(4):191–205. [PubMed: 15229932]

28. Ulrich EL, Akutsu H, Doreleijers JF, Harano Y, Ioannidis YE, Lin J, Livny M, Mading S, Maziuk D, Miller Z, Nakatani E, Schulte CF, Tolmie DE, Wenger RK, Yao H, Markley JL. BioMagResBank. Nucleic Acids Research. 2007; 36:D402–D408. [PubMed: 17984079]

29. Wishart DS, Knox C, Guo AC, Eisner R, Young N, Gautam B, Hau DD, Psychogios N, Dong E, Bouatra S, Mandal R, Sinelnikov I, Xia J, Jia L, Cruz JA, Lim E, Sobsey CA, Shrivastava S, Huang P, Liu P, Fang L, Peng J, Fradette R, Cheng D, Tzur D, Clements M, Lewis A, De Souza A, Zuniga A, Dawe M, Xiong Y, Clive D, Greiner R, Nazyrova A, Shaykhutdinov R, Li L, Vogel HJ, Forsythe I. HMDB: a knowledgebase for the human metabolome. Nucleic Acids Res. 2009; 37(Database issue):D603–10. [PubMed: 18953024]

30. Cloarec O, Dumas ME, Craig A, Barton RH, Trygg J, Hudson J, Blancher C, Gauguier D, Lindon JC, Holmes E, Nicholson J. Statistical total correlation spectroscopy: an exploratory approach for latent biomarker identification from metabolic ^{1}H NMR data sets. Anal. Chem. 2005; 77(5):1282–9. [PubMed: 15732908]

31. Askenasy N, Kushnir T, Navon G, Kaplan O. Differences in metabolite content between intact pancreases and their perchloric acid extracts. A 2D $^{1}H/^{31}P$ correlation NMR study. NMR Biomed. 1990; 3(5):220–6. [PubMed: 1705138]

32. Cheng LL, Ma MJ, Becerra L, Ptak T, Tracey I, Lackner A, Gonzalez RG. Quantitative neuropathology by high resolution magic angle spinning proton magnetic resonance spectroscopy. Proc. Natl. Acad. Sci. U S A. 1997; 94(12):6408–13. [PubMed: 9177231]

33. Futahashi Y, Komano J, Urano E, Aoki T, Hamatake M, Miyauchi K, Yoshida T, Koyanagi Y, Matsuda Z, Yamamoto N. Separate elements are required for ligand-dependent and -independent internalization of metastatic potentiator CXCR4. Cancer Sci. 2007; 98(3):373–379. [PubMed: 17270027]

34. Tarasova NI, Stauber RH, Michejda CJ. Spontaneous and Ligand-induced Trafficking of CXC-Chemokine Receptor 4. Journal of Biological Chemistry. 1998; 273(26):15883–15886. [PubMed: 9632631]

35. Cloarec O, Dumas ME, Trygg J, Craig A, Barton RH, Lindon JC, Nicholson JK, Holmes E. Evaluation of the orthogonal projection on latent structure model limitations caused by chemical shift variability and improved visualization of biomarker changes in ^{1}H NMR spectroscopic metabonomic studies. Anal. Chem. 2005; 77(2):517–26. [PubMed: 15649048]

36. Morse DL, Carroll D, Day S, Gray H, Sadarangani P, Murthi S, Job C, Baggett B, Raghunand N, Gillies RJ. Characterization of breast cancers and therapy response by MRS and quantitative gene expression profiling in the choline pathway. NMR Biomed. 2009; 22(1):114–27. [PubMed: 19016452]

37. Glunde K, Jie C, Bhujwalla ZM. Molecular causes of the aberrant choline phospholipid metabolism in breast cancer. Cancer Res. 2004; 64(12):4270–6. [PubMed: 15205341]

38. Thomas MA, Lipnick S, Velan SS, Liu X, Banakar S, Binesh N, Ramadan S, Ambrosio A, Raylman RR, Sayre J, DeBruhl N, Bassett L. Investigation of breast cancer using two-dimensional MRS. NMR Biomed. 2009; 22(1):77–91. [PubMed: 19086016]

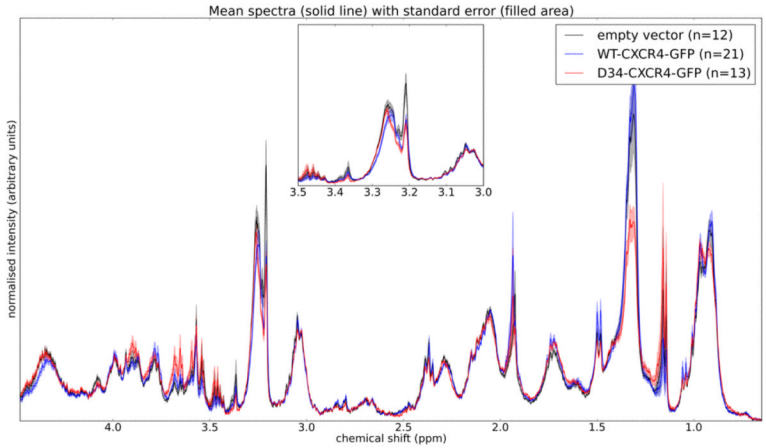

Figure 1.

Averaged and normalized ^{1}H HR-MAS spectra of lyophilised and rehydrated MTLn3E cells with empty vector (black), MTLn3E expressing WT-CXCR4-GFP (blue) and MTLn3 expressing Δ34-CXCR4-GFP (red). The coloured line represents the mean, shaded regions are the standard error. Spectra were normalized using PQN, with the median of the empty vector spectra as reference. Clear differences can be observed at 0.9 ppm, 1.33 ppm, 3.21 ppm and 3.66 ppm. The sample spinning rate was 5000 Hz and the samples were maintained at 37°C throughout the experiment.

Europe PMC Funders Author Manuscripts

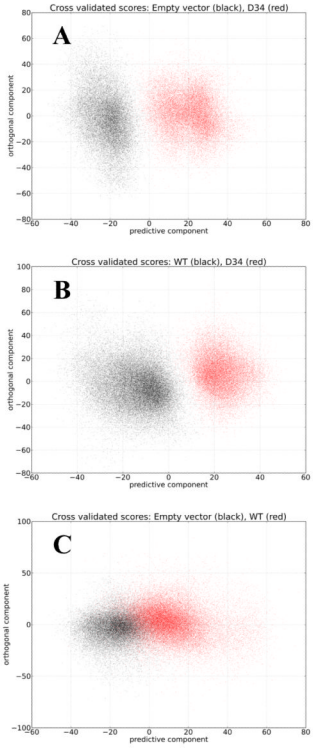

Figure 2.
PLS scores (after OPLS correction) of 2000 4-fold cross validation runs with randomly selected training and test sets for each run. A good classification is obtained where the truncation mutant is compared to any of the other two cell types. MTLn3E cells with an empty vector can also be separated from cells expressing WT-CXCR4-GFP, but the scores plot indicates that differences between these two cell types are less pronounced.

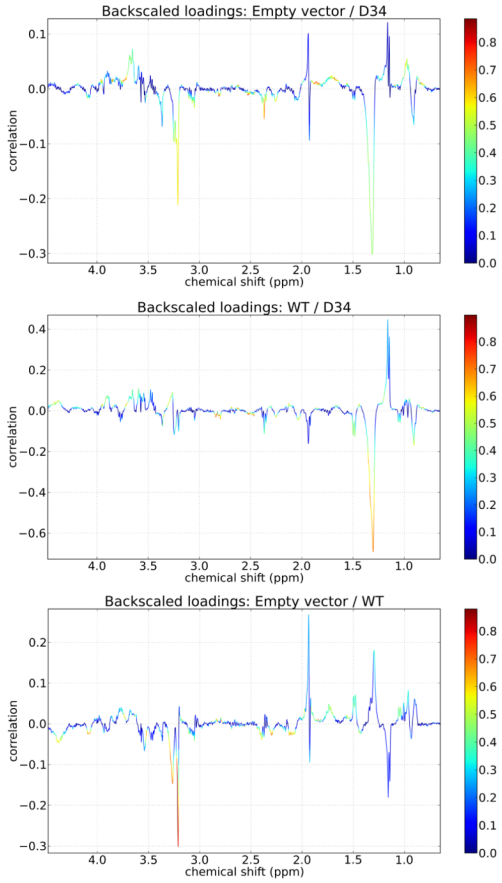

Figure 3.
Back-scaled loadings plots and weights give an overview of the ^{1}H resonance frequencies in ppm that allow the models to distinguish each of the two cell types under comparison.

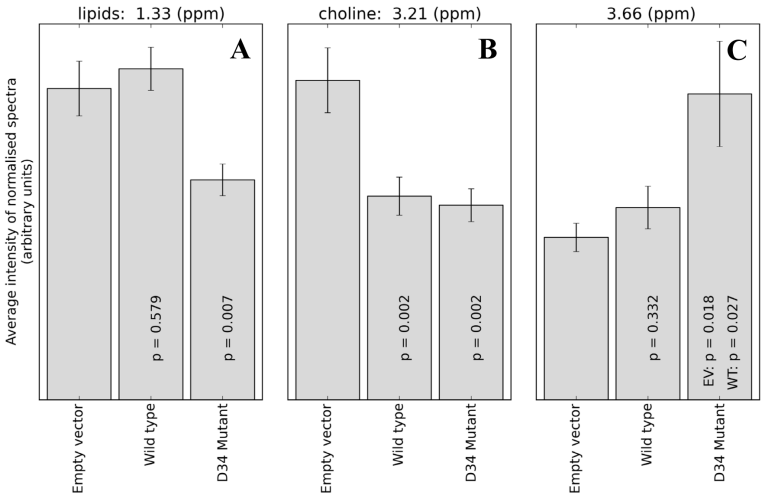

Figure 4.

Relative metabolite concentrations as determined by the area under the NMR spectrum at 1.33 ppm (assigned to lipids) (**A**), 3.21 ppm (assigned to choline) (**B**) and 3.66 ppm (**C**). Spectra were normalized using probabilistic quotient normalization using the median of the empty-vector spectra as reference, and averaged over the replicated experiments (empty vector: n=12, WT-CXCR4-GFP: n=21, Δ34-CXCR4-GFP: n=13. The *p*-values were calculated with respect to the signal from the cells expressing the empty vector, except for the truncation mutant at 3.66 ppm (**C**), where *p*-values with respect to cells transfected with empty vector (EV) and wild type (WT) are given. *p*-values were not corrected for multiple testing. Error bars are the standard error.